ACS OMEGA

Open Access

http://pubs.acs.org/journal/acsodf

Article

Evaluating the Effect of Resorcin[4]Arenes Conformational Structures on the Remediation of Methylene Blue in Water

Ali Husain,* Mohamed Rashad, Abrar Alrashed, Abdullah Alhendal, Maryam Jamali, and Saad Makhseed

Cite This: *ACS Omega* 2025, 10, 12014−12025

Read Online

ACCESS | Metrics & More | Article Recommendations | Supporting Information

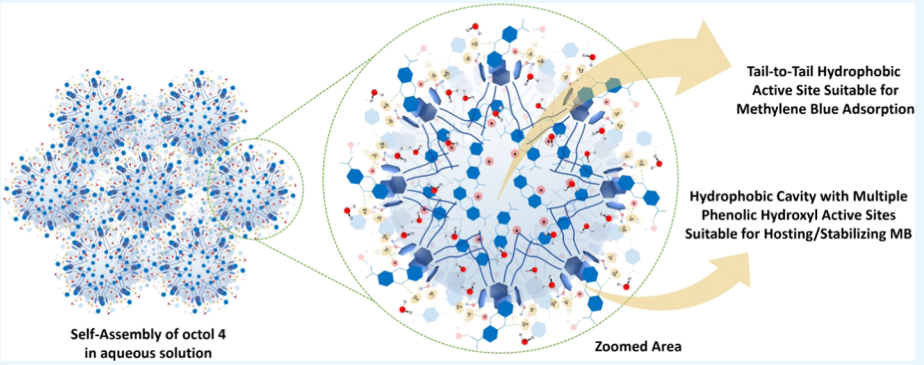

ABSTRACT: In this study, the effects of resorcin[4]arenes/cavitand structural properties: (i) hydrophobicity, aliphatic alkyl tails elongation (methyl, propyl, hexyl, and nonyl) based on macrocycles **1**−**4** lower rims; (ii) H-bond and dipole−dipole importance, resorcin[4]arene **4** vs its rigid core structure cavitand **5**; and (iii) cavity order/disorder, crown (C_{4v}) **4** vs chair (C_{2h}) **6** isomers on the remediation of methylene blue (MB) in water have been investigated. Additionally, the adsorption kinetics/isotherms of MB by octols **1**−**4** were studied, indicating that the adsorption process follows *pseudo*-second order and Langmuir models, respectively. Notably, the longest alkylated crown (C_{4V}) conformer **4** was found to be the best adsorbent among the studied macrocycle family with a remarkable adsorption capacity (Q_{max} = 769.230 mg/g), owing to its unique structural features and tail-to-tail aggregation behavior in water. Hence, resorcin[4]arene **4** was further used to evaluate its adsorption efficiency toward other (non)ionic dyes, and the results were considerable. Also, its recoverability/reusability toward MB removal from water was examined for five consecutive cycles, and the results revealed a promising recovering capability with excellent adsorption efficiency, leading to confidence in its effective use for manifold adsorption/desorption cycles.

INTRODUCTION

Since the industrial revolution, wastewater containing dye pollutants has become a major concern, leading to unexceptional impacts on the environment and human health.[1] Synthetic dyes are generally consumed worldwide by small to large industries, that is, the production of million tons all over the world in the tannery, food, cosmetic, textile, and pharmaceutical sectors.[2] Recent studies showed that about 12% of synthetic dyes are lost during manufacturing and processing, and 20% of the color enters the environment through industrial wastewater treatment plants. In general, the structural complexity of dye substrates, e.g., aromatic rings bearing different functionalities, rapid solubility in water (the presence of many polar and/or charged ionic sites),[3] nonbiodegradability (aromatic hydrocarbons stability),[4] excellent light absorption within 380−700 nm spectra (π-electron delocalization),[5] and extreme toxicity, e.g., dyes containing azo (−N=N−) groups has been highly carcinogenic due to amine and benzidine emissions, making these chromophores a high-risk contamination on both environment and living life.[6] Several treatment methods have been developed for removing and reducing the environmental impacts caused by dyes such as oxidative processes,[7] coagulation,[8] electrochemical,[9] biodegradation, and adsorption.[10] However, adsorption among the mentioned techniques has many benefits including simplicity, efficiency, cost-effectiveness, relatively low sludge output, etc., making it a convenient and reliable method for wastewater purification.[11]

Macrocyclic arenes (Figure 1), e.g., cyclotriveratrylene, calix[4]arenes, resorcin[4]arenes, and pillar[5]arenes,[12] have unique structural properties, making them an important class of molecular entities.[13]

Received: October 26, 2024
Revised: March 5, 2025
Accepted: March 14, 2025
Published: March 20, 2025

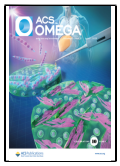

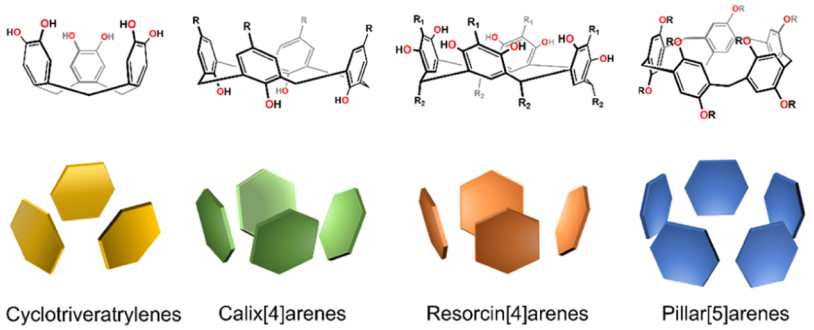

Figure 1. General structures of macrocyclic arenes.

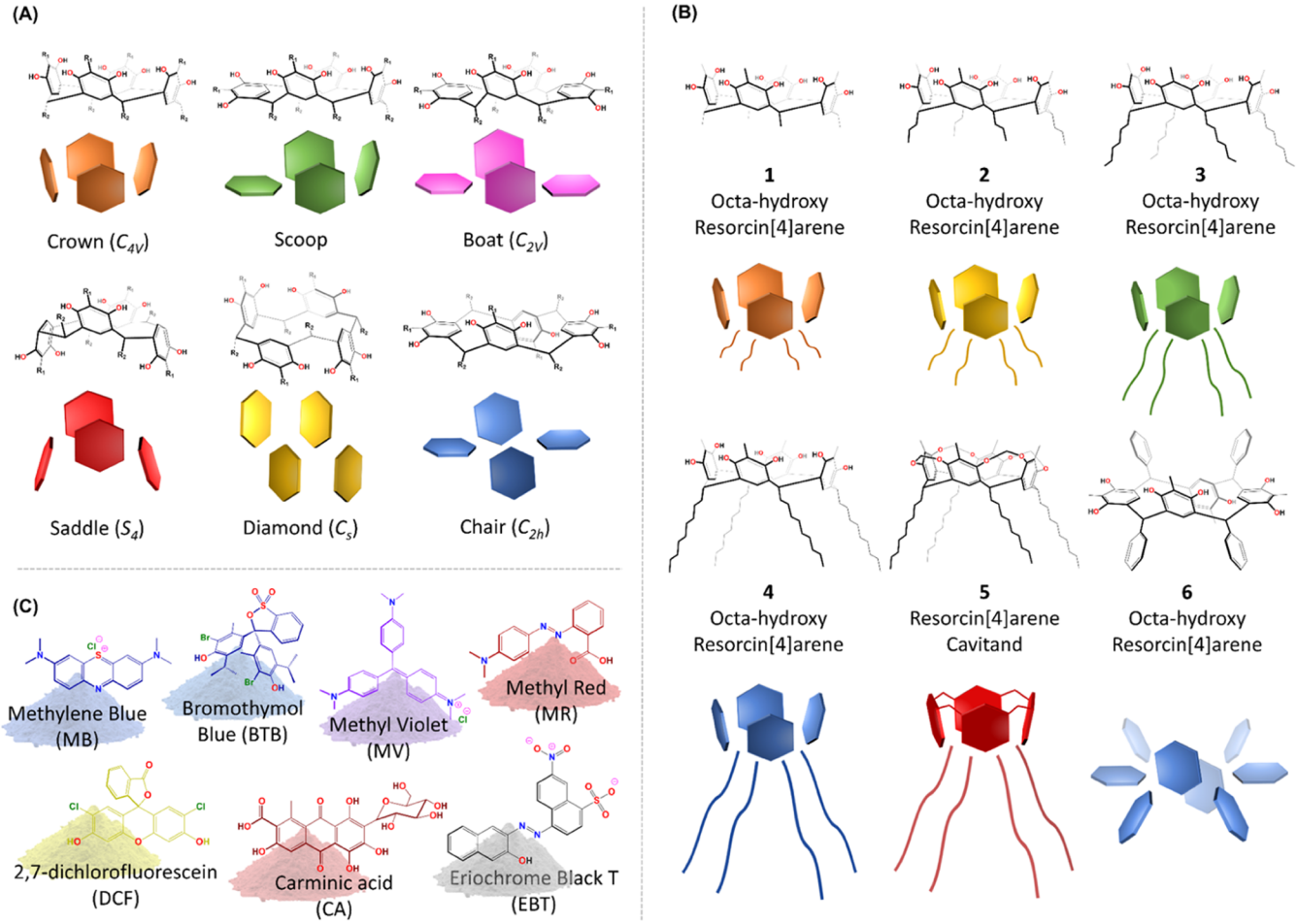

Figure 2. General structures of (A) resorcin[4]arenes conformational structures, (B) resorcin[4]arenes **1**−**4** & **6** and cavitand **5**, and (C) neutral/ionic dyes.

Among these identified macrocyclic hosts, resorcin[4]arenes, which were first achieved by Adolf Baeyer in 1872 from the acid-catalyzed cyclo-condensation reaction of resorcinol with benzaldehyde,[14] have since then attracted considerable and still growing attention in different research areas, specifically those associated with host−guest and supramolecular chemistry.[15]

Many conformational structures (Figure 2A), namely crown (C_{4v}),[16] boat (C_{2v}), chair (C_{2h}),[17] diamond (C_s),[18] saddle (S_4),[19] and scoop isomers,[20] can practically attained by these macrocycles. The (C_{4v}) conformer, known for its thermodynamic stability and semirigid structure, is the most standard and commonly utilized isomer in scientific literature due to multiple intramolecular hydrogen bonding interactions between adjacent hydroxyl groups.[21] Indeed, many applications have been established by the C_{4v} conformer including (i) starting materials for cavitands and (hemi)carcerands formations;[22] (ii) multivalent molecular platforms of spatial directionality appropriate for attaching and directing different ligating sites;[23] (iii) microvessels and ionophores (multiple phenols along with a hydrophobic interior cavity apposite for hosting a variety of (non)ionic species);[24] (iv) microreactors (π-electron rich cavity suitable for organic transformations and chemical catalysis);[25] and (v) supramolecular assemblies (dimeric/hexameric structures via noncovalent intermolecular interactions and metal complexations).[26] However, and to the best of our knowledge,

https://doi.org/10.1021/acsomega.4c09763
ACS Omega 2025, 10, 12014−12025

Scheme 1. Synthesis of Resorcin[4]Arenes, Crown (C_{4v}) Conformers 1-4, Cavitand 5, and Chair (C_{2h}) Isomer 6

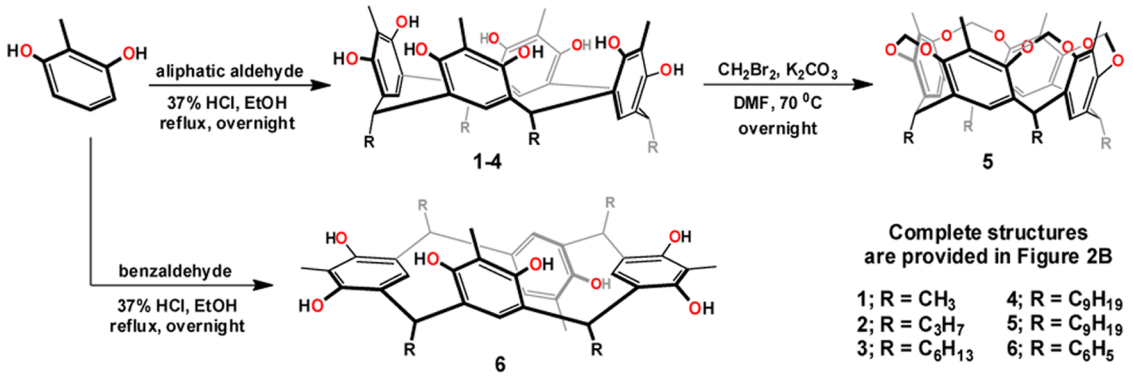

the use of these frameworks, especially in host−guest chemistry, has been limited to neutral and ionic substrate accommodation/stabilization and/or organic catalysis[27−29] and has never been reported in dye elimination from contaminated water. Accordingly, using the advantages of the presence of resorcin[4]arene structures, i.e., a well-defined hydrophobic cavity environment along with multiple H-bond donor−acceptor phenolic groups in dye removal from contaminated water, is worth to be evaluated.

Herein, the efficiency of resorcin[4]arenes/cavitand (**1**−**6**, Figure 2B) as molecular adsorbents for dye removal from aqueous media is described. The effects of the adsorbent structures: (i) hydrophobicity, aliphatic alkyl chains variation on macrocycles **1**−**4** lower rims (−CH_3, −C_3H_7, −C_6H_{13}, and −C_9H_{19}); (ii) presence/absence of H-bonding and (ion)dipole−dipole active sites, octol **4** vs cavitand **5**; and (iii) cavity (dis)order, crown (C_{4v}) **4** vs chair (C_{2h}) **6** on methylene blue (MB) removal from water have been investigated. A set of neutral and ionic dyes (Figure 2C) such as bromothymol blue (BTB), methyl violet (MV), methyl red (MR), 2,7-dichlorofluorescein (DFC), carminic acid (CA), and Eriochrome black T (EBT) have been involved in this study, and their remediation from water using macrocycle **4** has been evaluated. In addition, the capability of octol **4** as an efficient recoverable/reusable adsorbent toward MB removal from water was examined for five consecutive adsorption/desorption cycles.

RESULTS AND DISCUSSION

Synthesis of Resorcin[4]Arenes/Cavitand, Crown (C_{4v}) Conformers 1−4, Cavitand 5, and Chair (C_{2h}) isomer 6. A family of four octa-hydroxy resorcin[4]arenes in their crown (C_{4v}) conformers **1**−**4** bearing different length aliphatic chains on their lower core structures, namely methyl, propyl, hexyl, and nonyl, have been successfully synthesized via the traditional acid-catalyzed condensation reaction of methyl resorcinol with various aliphatic aldehydes. All cyclic tetramers **1**−**4** were obtained in gram quantities (79−83%) by treating 2-methyl resorcinol with ethanal, butanal, heptanal, and decanal, respectively, in the presence of a catalytic amount of 37% HCl in refluxing ethanol (Scheme 1).[30]

The aim of fluctuating the alkyl groups on the lower rim of compounds **1**−**4** is to evaluate the hydrophobic effect on the removal of MB from water. Moreover, macrocycle **4** was further locked into its rigid "chalise" shape, cavitand **5**, to examine the outcome of phenolic group termination on MB adsorption from water as compared to its corresponding starting material, macrocycle **4**. Cavitand **5** was achieved in a high yield (87%) by bridging the adjacent hydroxyls with methylene linkers upon the reaction of octol **4** with dibromomethane in the presence of potassium carbonate in DMF at 70 °C (Scheme 1). Furthermore, to investigate the role of the cavity system existing in crown (C_{4v}) conformer **4** on MB elimination from water, chair (C_{2h}) isomer **6**, which lacks the cavity order within its macrocyclic skeleton, was prepared. Octol **6** was obtained in 89% from the cyclo-tetramerization reaction of an ethanolic solution of 2-methyl resorcinol with benzaldehyde in the presence of 37% HCl (Scheme 1). The structures of all compounds **1**−**6** were well-established from their respective NMR, FT-IR, DSC, and HRMS spectral data. The related spectra are provided in the Supporting Information section (SI). The conformational dynamics of the studied resorcin[4]arene derivatives could be further explored using variable-temperature nuclear magnetic resonance (VT-NMR). However, the insolubility of these compounds in water presents a significant challenge for such investigations. While alternative solvents such as DMSO-d_6 or $CDCl_3$ could be used for VT-NMR studies,[31,32] it is well-known that changes in the solvation environment can significantly influence molecular conformations, intermolecular interactions, and the host−guest complexation process.[33]

Optimizing the Adsorption Parameters of MB from Aqueous Media Using Octols 1−4. Initially, the equilibrium, kinetics, and thermodynamics features of the adsorption process were demonstrated upon evaluating the effect of pH variation, contact time, and adsorbent dosage on MB substrate elimination from water using macrocycles **1**−**4**. These parameters would provide the ideal adsorbent structure upon investigating the influence of the hydrophobic alkyl tails variation on MB elimination, as well as the best adsorption condition applied for further studies.

Effect of the Aliphatic Alkyl Chains Elongation Based on Octols 1−4 Lower Rims on MB Removal from Aqueous Media. The hydrophobic effect based on the aliphatic alkyl chain elongation existing in octols **1**−**4** on MB adsorption was investigated under the following adsorption condition: MB = 10 mg/L, contact time = 1440 min, adsorbent dosage = 50 mg, and pH = 7 at 25 °C. Interestingly, it was found that varying the length of the hydrophobic tails based on the macrocyclic lower rims has a significant impact on the adsorption process in which the adsorption yields were effectively increased with extending the length of the alkyl chains, that is, 77.7, 91.7, 95.8, and 97.9% for octols **1**−**4**, respectively (Figure 3A). The poor adsorption yield of MB afforded by octol **1** can be elucidated by its slight solubility in water owing to its high hydrophilic character (multiple phenols

https://doi.org/10.1021/acsomega.4c09763
ACS Omega 2025, 10, 12014−12025

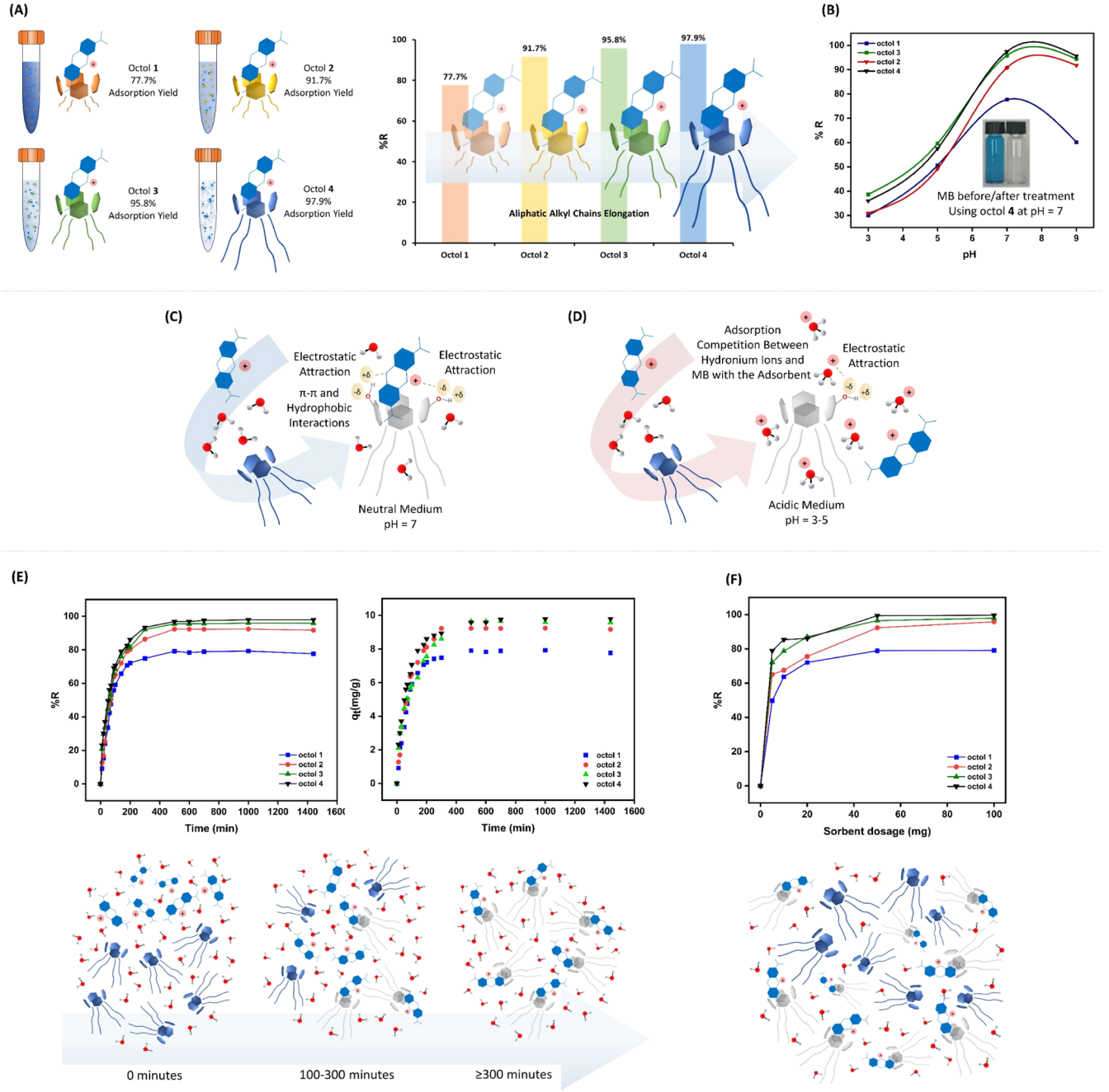

Figure 3. (A) Adsorption yields of MB removal from aqueous solutions using octols **1**−**4**. (B) Influence of pH on the adsorption of MB by octols **1**−**4**. Proposed adsorption mechanism of MB by octol **4** in (C) neutral (pH = 7) and (D) acidic (pH = 3−5) media. (E) Effect of contact time on the adsorption of MB by octols **1**−**4** and (F) effect of adsorbent dosage on the adsorption of MB by octols **1**−**4**.

vs short alkyl tails) as compared to the longer alkylated structures **2**−**4**. Hence, replacing the methyl groups presented in macrocycle **1** with longer aliphatic chains such as propyl, hexyl, and nonyl in octols **2**−**4** elevates their structural hydrophobicity, and thus, lower solubility in water along with higher adsorption ability toward MB has been accomplished.

Effect of Initial pH on the Adsorption of MB from Aqueous Media Using Octols 1−4. Manipulating the surface charges of the adsorbents upon varying the pH value of the solution has a considerable influence on the adsorption process. The impact of pH on MB removal was therefore studied at different levels, pH = 3, 5, 7, and 9. All measurements were performed in triplicate, and the average amount of MB removed was calculated to ensure the reliability and reproducibility of the results (Figure 3B). The results show that the highest adsorption yields were achieved at pH = 7 for all studied macrocycles (Figure 3C). On the other hand, lowering the pH value from pH = 7 to 3 resulted in a decrease in MB adsorption, that is, from 77.7 to 30.1% for **1**, 91.7 to 35.6% for **2**, 95.8 to 38.7% for **3**, and 97.9 to 40.3% for **4**. Such reduction in the adsorption efficacy can be clarified by increasing the concentration of hydronium ions (H_3O^+) in acidic media that may compete with the cationic MB for free active zones on the adsorbent structures (Figure 3D).[34] No impact on the solubility of the studied structures (octols 1−4) in water at pH 3−5 has been detected. However, at a higher pH value (pH 9), octol 1 was completely soluble in

https://doi.org/10.1021/acsomega.4c09763
ACS Omega 2025, 10, 12014−12025

Table 1. Parameters of Kinetic Models of MB Adsorption by Octols 1-4

		octol 1	octol 2	octol 3	octol 4
pseudo-first order	$q_{e,\ exp}$ (mg/g)	7.93	9.24	9.7	9.8
	k_1 (min^{-1})	0.0071	0.0088	0.0044	0.0065
	$q_{e,\ cal}$ (mg/g)	5.27	7.1	5.6	6.1
	R^2	0.988	0.9976	0.920	0.987
pseudo-second order	k_2 (g/mg·min)	2.62×10^{-3}	2.57×10^{-3}	2.62×10^{-3}	2.01×10^{-3}
	$q_{e,\ cal}$ (mg/g)	8.37	9.7	10.37	10.43
	R^2	0.9993	0.9990	0.9986	0.9999
Elovich equation	α (mg/g·min)	8.241	19.362	5.984	3.659
	β (g/mg)	1.699	2.075	1.836	1.816
	R^2	0.9363	0.9354	0.9839	0.9684
intraparticle diffusion model	k_{id} (mg/g·$h^{0.5}$)	1.70587 ± 0.12617	1.95219 ± 0.16134	1.93758 ± 0.09707	2.08491 ± 0.09558
	C (mg/g)	$8.91549 \times 10^{-16} \pm 0$	$1.16957 \times 10^{-15} \pm 0$	$1 \times 10^{-14} \pm 0$	$1 \times 10^{-14} \pm 0$
	R^2	0.81765	0.79834	0.88104	0.90394

water, while octols 2−4 remained insoluble. Additionally, complete studies examining the effects of contact time, adsorbent dosage, and pH value on the adsorption process were conducted exclusively on crown conformers 1−4 but not on cavitand 5 or chair conformer octol 6. Moreover, at pH 9, the effectiveness of methylene blue (MB) removal was slightly reduced by octols 2−4, while a significant decrease of 15% was observed when the shortest alkylated octol 1 was used. This reduction can be attributed to its complete solubility in solution at this pH, limiting its adsorption efficiency.

Aqueous Media Using Octols 1−4. Figure 3E illustrates the effect of contact time on MB elimination by octols **1**−**4** over a period ranging from 0 to 1440 min with a fixed initial dye concentration of 10 mg/L, pH = 7, and 25 °C. From the results, a rapid uptake of MB was observed in the first 100 min, followed by a slower adsorption rate until saturation was completed. At this point, the amount of adsorbed MB dyes reached a dynamic equilibrium state with the amount of dyes in the solution.[35] The time taken to complete this equilibrium stage is referred to as the equilibrium time, which represents the maximum MB uptake under the experimental conditions used. Besides, a rapid adsorption rate was achieved at the initial stage owing to the adsorbent's vacant active sites availability, which are parallelly occupied MB molecules with time.[36] Though, after a certain time, the remaining untenanted sites became difficult to engage in the adsorption process because of the possible repulsive forces between the solute molecules on the solid/bulk phases.

Effect of Adsorbent Dosage on the Adsorption of MB from Aqueous Media Using Octols 1−4. To examine the impact of adsorbent **1**−**4** dosage on MB removal, adsorbent amounts ranging from 20 to 100 mg have been conducted under similar adsorption conditions used previously. As shown in Figure 3F, raising the adsorbent dosage from 20 to 100 mg led to an increase in the adsorption yields, i.e., 37.1 to 80.1%, 47.6 to 95.8%, 52.2 to 98.0%, and 65.2 to 99.6% for octols **1**−**4**, respectively. All measurements were conducted in triplicate, and the average amount of MB removed was calculated to ensure the accuracy and consistency of the results. Clearly, this enhancement in MB adsorption is due to the increasing number of binding sites attained by adsorbent enrichment in solution.

Adsorption Kinetics. To validate the adsorption mechanism of MB onto macrocycles **1**−**4**, kinetic models including *pseudo*-first-order, *pseudo*-second-order, Elovich, and intraparticle diffusion have been studied (SI).[37] The kinetic model parameters are summarized in Table 1. The results indicate that the *pseudo*-second-order model is a better fit for describing the adsorption mechanism of MB by the studied adsorbents **1**−**4**. Complete data are provided in the Supporting Information section (SI). It was observed that the adsorption capacity (q_e) generally increases with chain length; however, this increase is not as pronounced as initially expected. This behavior can be attributed to two main factors: (i) saturation of adsorption sites as the chain length increases and (ii) steric hindrance, which may reduce the accessibility of adsorption sites.[38−40]

Adsorption Isotherms. Several isotherm models are available in the literature, and for equilibrium result evaluation, three commonly used models, that is, Langmuir, Freundlich, and Temkin isotherms,[41] were selected (SI). The results for each model are presented in Table 2. From the results, it was

Table 2. Isotherm Parameters of MB Adsorption by Octols 1-4

model		octol 1	octol 2	octol 3	octol 4
Langmuir	Q_{max} (mg/g)	41.84	70.92	250.00	769.23
	R_L	0.247	0.735	0.454	0.536
	R^2	0.994	1	1	0.999
Freundlich	K (mg/g)	10.530	90.614	385.390	1186.040
	n	0.961	0.859	0.994	1.039
	R^2	0.999	0.975	0.999	0.988
Tempkin	A (mg/L)	1.876	1.160	2.782	3.900
	B	8.814	24.825	17.674	20.026
	R^2	0.782	0.934	0.885	0.920

indicated that the Langmuir isotherm model fits suitably for the adsorption process of MB from water by the studied structures **1**−**4**. Complete data are provided in the Supporting Information section (SI).

Remarkably, it was determined from the results that the adsorption capacity was amplified by the aliphatic chain lengths, i.e., Q_{max} (mg/g) = 41.84, 70.92, 250.00, and 769.23 for octols **1**−**4**, respectively. This spectacular increase in the adsorption process can be expressed by the ability of the studied adsorbents to self-assemble via tail-to-tail aggregation in water,[40,42,43] which can be controlled by manipulating the length of the hydrophobic tails based on the macrocycle lower rims. To support this hypothesis, scanning electron microscopy (SEM) was used to study the surface morphology of macrocycles **1**−**4** before/after the adsorption of MB substrates (Figure 4A−H). Evidently, the surface morphology of the adsorbents has notably changed, and by means of this, the surface became smoother, which indicates the adsorption of MB by the adsorbents.

https://doi.org/10.1021/acsomega.4c09763
ACS Omega 2025, 10, 12014−12025

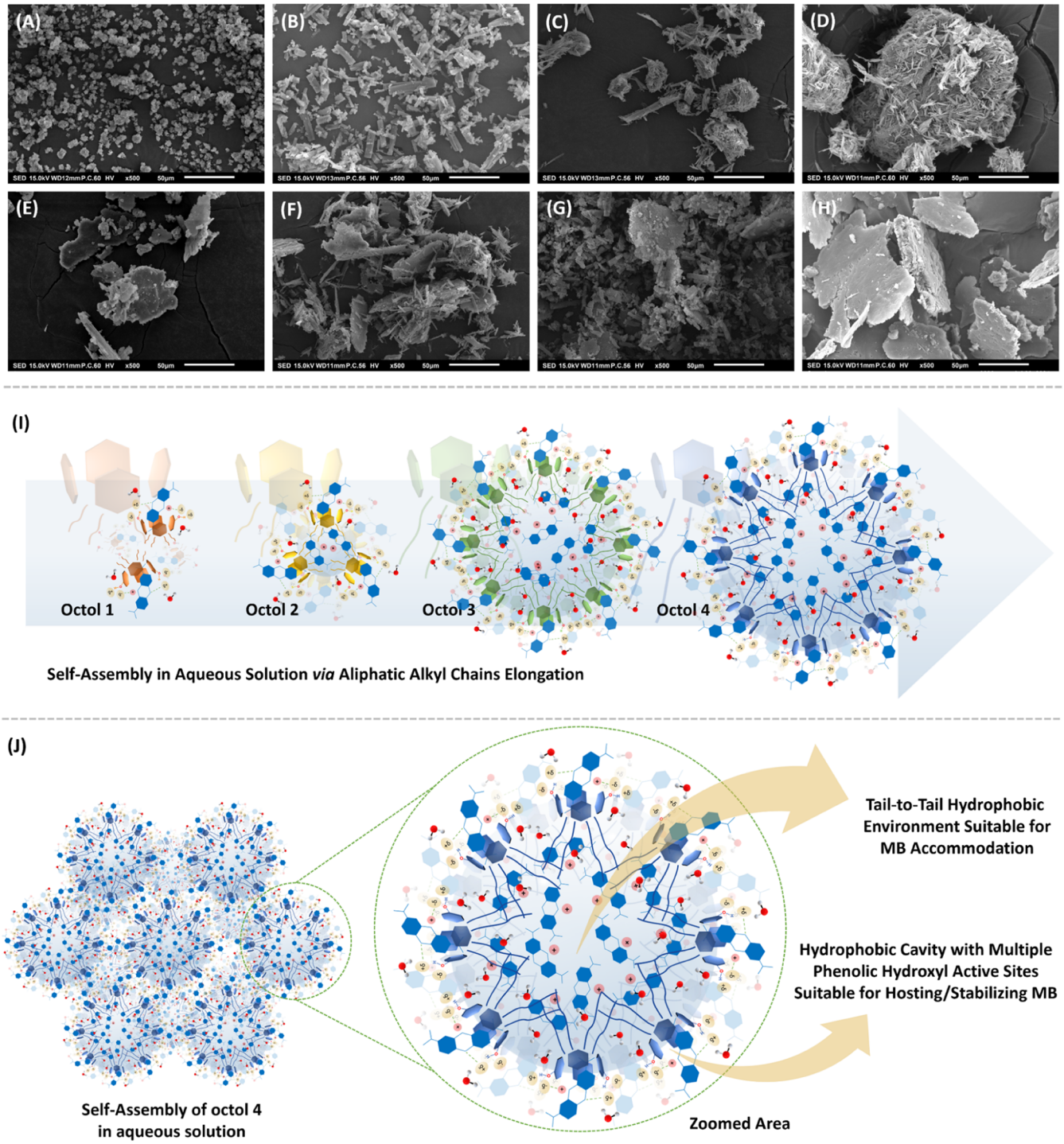

Figure 4. SEM images of octols **1**−**4** (A−D) before the adsorption of MB and (E−H) after the adsorption of MB, magnification x500. (I) Proposed tail-to-tail self-assembly by octols **1**−**4** and (J) Octol 4 active sites (hydrophobic cavity, multiple phenols, and hydrophobic environment based on tail-to-tail aggregation).

Furthermore, a clear indication of self-assembled materials has been detected by monitoring the adsorbents **1**−**4** size variations; that is, the size of the material became larger as the length of the hydrophobic tails became longer (Figure 4I). Macrocycle **4** that has the longest alkyl chains on its lower core was found to have the highest adsorption capacity, Q_{max} (mg/g) = 769.23, suggesting that the aliphatic networks resulted from the tail-to-tail self-assembly in solution, and not only the upper rim active sites (cavity system and multiple phenolics groups) have a significant role in providing a suitable hydrophobic environment for MB in water (Figure 4J). A comparison between the results attained in this work and those of other reported adsorbents on MB dye removal from aqueous media is presented in Table S1.

Real Sample Application. Tap water was used to examine the applicability of macrocycles **1**−**4** for MB adsorption in real samples. For this purpose, a certain amount of dye was added into real samples to prepare a 10 mg/L MB neutral solution, and adsorption experiments were carried out in 10, 50, 200, and 400

https://doi.org/10.1021/acsomega.4c09763
ACS Omega 2025, 10, 12014−12025

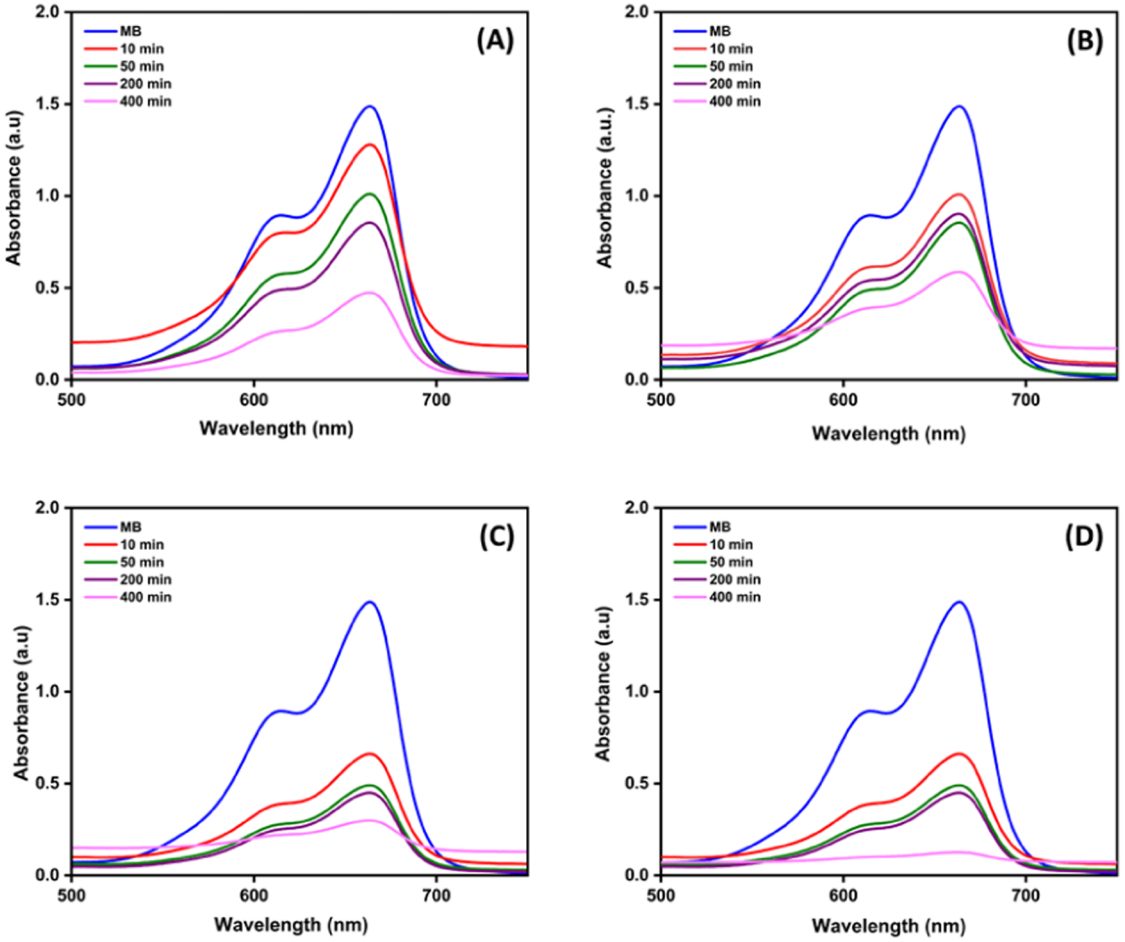

Figure 5. UV−Vis spectra for MB adsorption by octols (A) **1**, (B) **2**, (C) **3**, and (D) **4** in tap water.

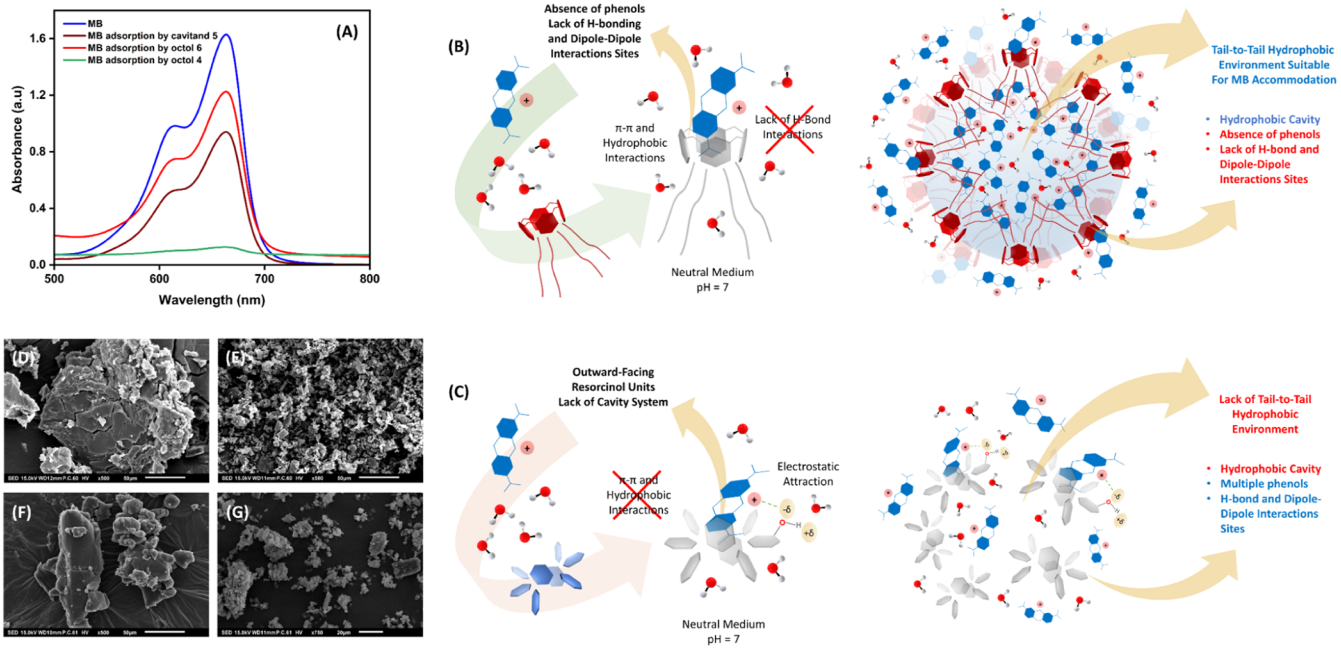

Figure 6. (A) UV−vis spectra for MB adsorption by octol **4**, cavitand **5**, and octol **6**. Proposed adsorption mechanism of MB by (B) cavitand **5** and (C) octol **6**. (D, E) SEM images of cavitand **5** and octol **6** before and (F, G) after adsorption of MB, magnification x500.

min at 25 °C. From the ultraviolet−visible (UV−vis) spectra, Figure 5, it was found that the adsorption yield of MB was lower in real samples compared with the results obtained previously when deionized water was used. The decrease in MB adsorbate

https://doi.org/10.1021/acsomega.4c09763
ACS Omega 2025, 10, 12014−12025

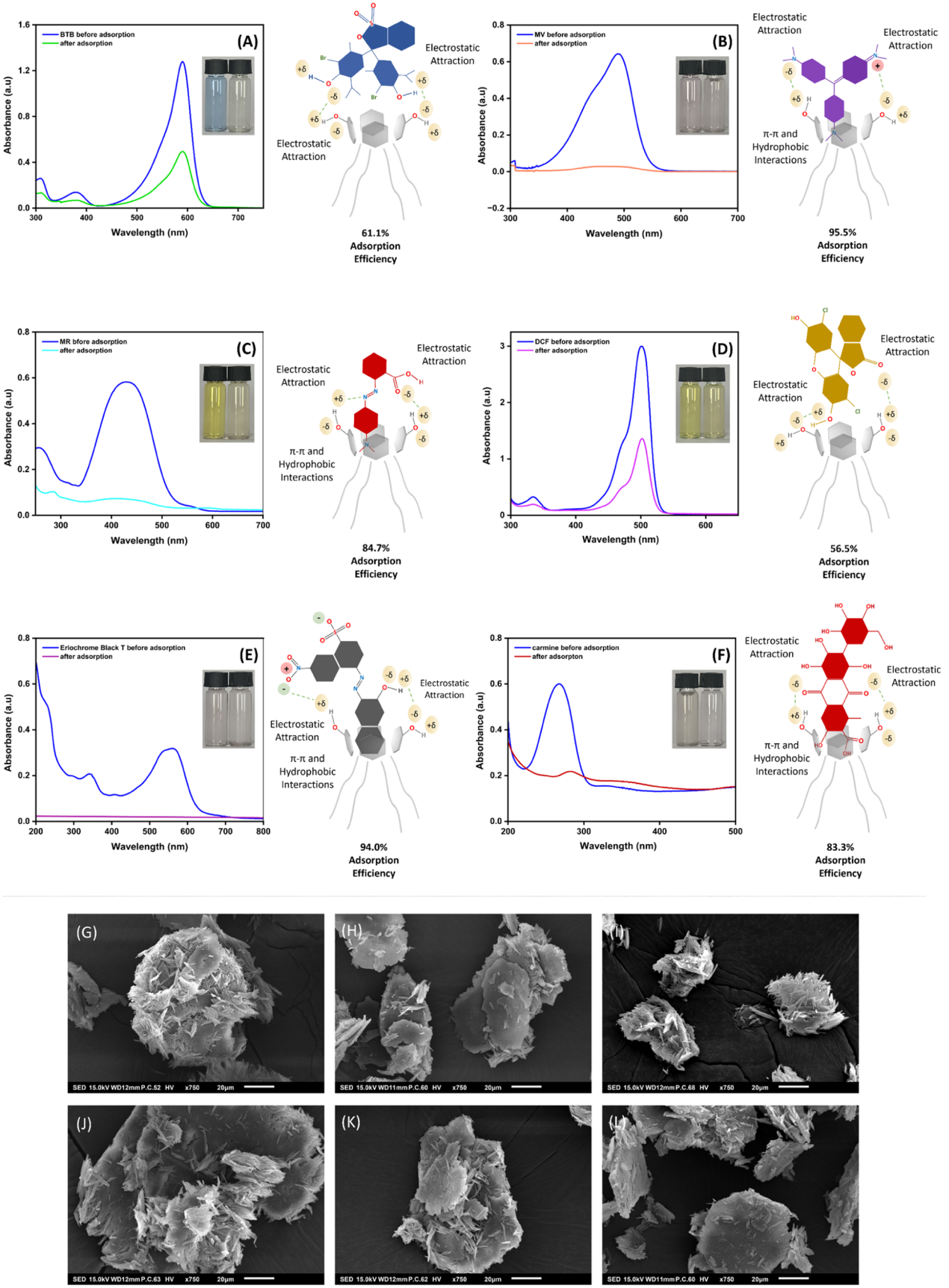

Figure 7. UV−vis spectra of (A) BTB, (B) MV, (C) MR, (D) DFC, (E) EBT, and (F) CA after treatment with octol **4**. SEM images of octol **4** after the adsorption of (G) BTB, (H) MV, (I) MR, (J) DFC, (K) EBT, and (L) CA, magnification ×750.

https://doi.org/10.1021/acsomega.4c09763
ACS Omega 2025, 10, 12014−12025

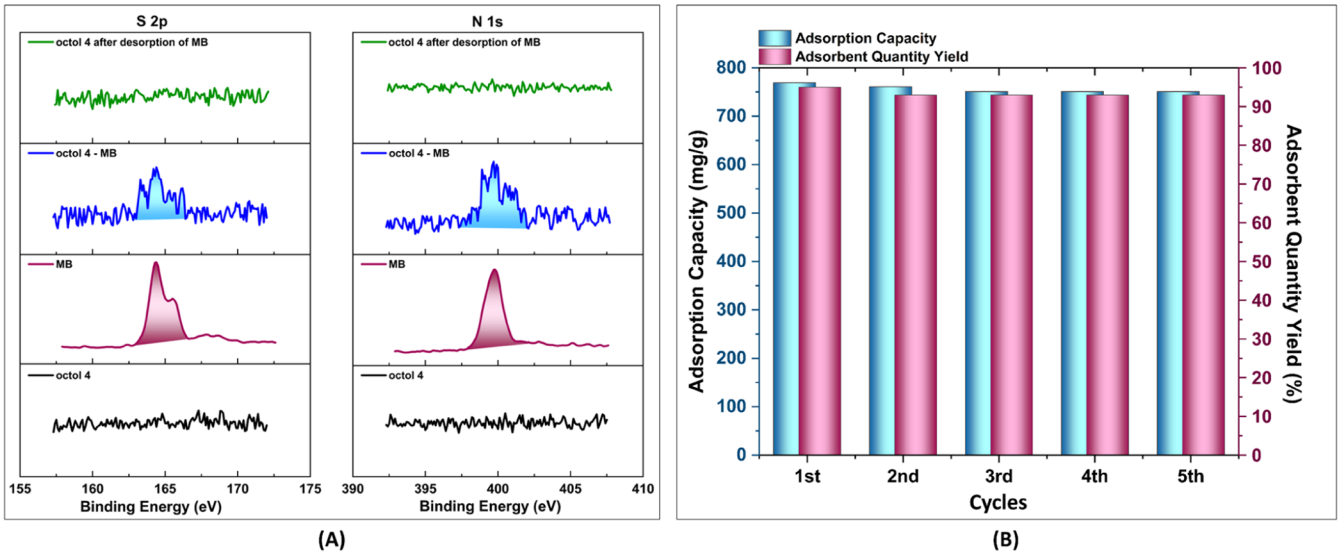

Figure 8. (A) XPS spectra of S 2p and N 1s of octol **4** (black), MB (purple), octol **4** − MB (blue), and octol **4** after desorption of MB dye (green) and (B) regeneration studies of MB dye adsorption over octol **4**.

removal is due to the interaction of the studied adsorbents with the ionic contaminations presented in tap water that compete with MB substrate on the active sites based on the adsorbent structures.[44]

Evaluating the Effect of Phenols Termination, Octol 4 vs Cavitand 5, and Cavity Order/Disorder, Crown (C_{4v}) 4 vs Chair (C_{2h}) 6 Conformers, on MB Adsorption from Aqueous Media. Reaching this point of success in demonstrating the best adsorption condition as well as identifying the ideal adsorbent, octol **4**, for MB removal from water, the effect of the adsorbent structure, i.e., the absence of H-bond and dipole−dipole active sites in cavitand **5** along with the lack of cavity order in octol **6** on the adsorption process, was examined following the typical adsorption condition used in MB adsorption study (Figure 6A).

From the results, it was determined that the crown (C_{4v}) **4** has the maximum adsorption yield (97.7%) as compared to cavitand **5** (35.4%) and chair (C_{2h}) isomer **6** (15.5%), suggesting that all structural features including (i) a semirigid cavity, (ii) multiple phenolic groups, along with (iii) long aliphatic chains existing in octol **4** have an important role in hosting/stabilizing MB in water. Indeed, the resulting rigid core in cavitand **5** still offers a suitable hydrophobic cavity and long aliphatic alkyl tails for aggregation purposes. However, the lack of H-bond donor−acceptor stabilizing agents within its backbone structure after terminating the multiple phenolic hydroxyls with methylene linkers diminished its effectiveness toward MB molecules in aqueous solution (Figure 6B). Furthermore, the notable reduction in the adsorption capability of octol **6** (15.5%) supports the hypothesis of the cavity order importance that exists in octol **4** in which the chair (C_{2h}) isomer, which consists of outward-facing resorcinol units within its skeleton, lacks a suitable lumen environment for MB accommodation. However, other nonbonding interactions such as H-bond/dipole−dipole forces may contribute to the adsorption process by the attraction between the hydroxyl groups presented in octol **6** with the positive charge on the MB center (Figure 6C). Additionally, SEM was further used to confirm the surface morphology of the studied structures before and after the adsorption of MB (Figure 6D−G). A noticeable smoothness of cavitand **5** surface after the adsorption process (Figure 6E) has been obtained, indicating the partial adsorption of MB (35.4%), while no significant changes on the surface morphology of octol **6** were detected (Figure 6G), signifying its poor adsorption toward MB in solution (15.5%).

Scoping the Adsorption Effectiveness of Octol 4 toward Different Neutral/Ionic Dyes from Aqueous Solutions. Next, the ability of octol **4** as a molecular adsorbent capable of removing contaminated materials from aqueous media was explored toward different neutral/ionic dyes, including bromothymol blue (BTB), methyl violet (MV), methyl red (MR), 2,7-dichlorofluorescein (DFC), carminic acid (CA), and Eriochrome black T (EBT). All adsorption studies were accomplished using similar adsorption conditions subjected to MB elimination, i.e., adsorbate initial concentration = 10 mg/L, contact time = 1440 min, adsorbent dosage = 50 mg, and pH = 7, at 25 °C (Figure 7A−F). From the results, excellent removal of CA, MR, EBT, and MV from aqueous solutions was achieved, i.e., 83.3% for CA, 87.7% for MR, 94.0% for EBT, and 95.5% for MV, while lower adsorption efficiencies were attained for DCF (56.5%) and BTB (61.1%). The significant adsorption of CA, MR, EBT, and MV adsorbates is due to their strong binding affinity toward various attraction forces with the macrocyclic active sites, i.e., inclusion complex within the adsorbent hydrophobic cavity and H-bond and/or (ion)dipole−dipole stabilizations by the phenolic sites. Indeed, favorable dipole−dipole interaction between DCF and BTB dyes with the adsorbent hydroxyl groups may contribute to their elimination from water. However, their low adsorption, i.e., 56.5% for DCF and 61.1% for BTB, is due to their structural rigidity that may interrupt their host−guest complex formation with the adsorbent interior cavity. SEM was also used to validate the adsorption process of all dyes by octol **4** (Figure 7G−L).

Adsorption/Desorption Studies of MB by Octol 4 Using XPS. XPS was applied to confirm the adsorption−desorption of MB upon determining the changes in the S 2p and N 1s signals in the XPS spectra (Figure 8A). Initially, the XPS data of a freshly prepared macrocycle **4** sample revealed no signals in the S 2p and N 1s regions, while strong signals corresponding to sulfur (S 2p) and nitrogen (N 1s) for the MB

https://doi.org/10.1021/acsomega.4c09763
ACS Omega 2025, 10, 12014−12025

sample were detected. Moreover, successful adsorption of MB by adsorbent **4** has been confirmed by the appearance of strong signals in the S 2p and N 1s areas in the XPS spectra of the resulting material, octol **4** − MB, which are attributed to sulfur and nitrogen in the MB substrate. Interestingly, the S 2p and N 1s signals completely disappeared from the XPS spectra after subjecting the material to methanol washing and centrifugation, authenticating the desorption of MB from the adsorbent structure.

Recoverability/Reusability of Octol 4 toward MB. Octol **4** underwent five consecutive adsorption/regeneration cycles upon washing the acquired material after the adsorption experiment with methanol solvent and centrifugation, followed by subjecting the recovered adsorbent **4** to the next adsorption cycle (Figure 8B). The results show a slight decrease in the maximum adsorption ability of MB over octol **4** with each successive cycle, e.g., the initial adsorption yield of a freshly used macrocycle **4** was 769.230 mg/g, which was reduced to 750 mg/g after completing the fifth adsorption cycle. Despite this reduction, macrocyclic structure **4** exhibited a promising recycling capability with excellent adsorption efficiency, leading to confidence in its effective use for multiple adsorption and desorption cycles in dye removal from contaminated water.

MATERIALS AND METHODS

Materials and Equipment. Methyl resorcinol, ethanal, butanal, heptanal, decanal, benzaldehyde, hydrochloric acid (37%), ethanol, dimethylformamide (DMF), dibromomethane, ethyl acetate, hexane, potassium carbonate, sodium sulfate, hydrochloric acid (37%), dyes including methylene blue (MB), bromothymol blue (BTB, 95%), methyl violet (MV), methyl red (MR), carminic acid (CA), and Eriochrome black T (EBT) were purchased from Sigma-Aldrich.

General Procedure for the Synthesis of Resorcin[4]-Arenes 1−4 and 6. 2-Methyl resorcinol (10.0 mmol) was dissolved in 80 mL of ethanol and 18.5 mL of 37% aqueous HCl. The solution was cooled in an ice bath, and aldehyde (10.0 mmol) was added slowly in a 10 min period. The reaction mixture was stirred at 0 °C for 5 min, which was then refluxed for 12 h. The precipitated compound resulting from the reaction was filtered out using a Buchner funnel and washed several times with cold ethanol and distilled water. The product was collected and dried in a vacuum oven at 40 °C.

General Procedure for the Synthesis of Cavitand 5. Octa-hydroxy resorcin[4]arene 4 (5 g, 4.8 mmol) was dissolved in 110 mL of DMF. Potassium carbonate (10.5 g, 76.3 mmol) was added into the solution and stirred for 10 min at room temperature. Dibromomethane (5.4 mL, 76.3 mmol) was then added, and the reaction mixture was heated to 70 °C overnight. The reaction mixture was monitored by TLC using (1:9) ethyl acetate/hexane. After completion, the reaction mixture was cooled at room temperature, and the obtained salt was filtered out using a Buchner funnel. The collected mixture was diluted in 200 mL of water and extracted using 100 mL of ethyl acetate, which was then washed with water (3 × 100 mL). The organic phase was collected and dried over Na_2SO_4.

MB Adsorption Capability from Aqueous Media. The batch adsorption method was utilized to adsorb MB on cyclic oligomers 1−4. To prepare the test solution, 500 mg of MB dye was dissolved in 500 mL of distilled water. For all experiments, a dilution of 10 mg/L was used. The experiments were carried out in an Erlenmeyer flask, where 50 mg of adsorbent and 50 mL of MB solution (10 mg/L) were mixed and stirred at 25 °C and pH 7. The mixture was centrifuged, and the solution in the supernatants was analyzed at 663 nm using a UV−vis spectrophotometer.

CONCLUSIONS

In conclusion, a family of six macrocycles, i.e., variable alkyl-tailed crown (C_{4v}) conformers **1**−**4**, cavitand **5**, and chair (C_{2h}) isomer **6**, have been used as molecular adsorbents toward dye removal from aqueous media. The ideal adsorption condition was established by evaluating the effect of pH variation, contact time, and adsorbent dosage on the adsorption process of MB from water using adsorbents **1**−**4**. The adsorption kinetics and isotherms were also studied, and the results reveal that the adsorption process of MB by octols **1**−**4** follows *pseudo*-second order and Langmuir models, respectively. Additionally, the effects of (i) hydrophobicity, aliphatic chain variation based on octols **1**−**4** lower rims; (ii) H-bond and (ion)dipole−dipole terminations, octol **4** vs cavitand **5**; and (iii) cavity (dis)order, crown (C_{4v}) **4** vs chair (C_{2h}) **6** isomers on MB removal have been evaluated. Valuable information associated with the macrocyclic structures was achieved, revealing that the combination of (i) long aliphatic tails, (ii) multiple phenolic groups, and (iii) a well-defined cavity system has a significant impact on the MB adsorption process. Resorcin[4]arene **4**, which exhibits all of these structural features, was found to be the best molecular adsorbent with an outstanding adsorption capacity of Q_{max} = 769.230 mg/g, owing to its unique tail-to-tail self-assembly behavior in aqueous media. Furthermore, the efficiency of macrocycle **4** was further examined with other neutral/ionic dyes, and the results were considerable. In addition, excellent recoverability/reusability of octol **4** toward MB removal from water was accomplished, i.e., five consecutive cycles, leading to confidence in its effective use for multiple adsorption/desorption cycles.

From the results, there are many advantages over other complexed structures reported in the literature, such as (i) preparation simplicity, that is, a single-step process with high-yielding desired products, (ii) dual active adsorbing/stabilizing sites, i.e., host−guest cavity system with multiple phenolic hydroxyl groups, (iii) sizable hydrophobic environment based on tail-to-tail aggregation process suitable for accommodating a variety of neutral guests and ionic species, and (iv) remarkable recoverability and reusability that make C_{4v} resorcin[4]arenes suitable adsorbent templates for removing contaminated materials from water. Such an approach, thus, is essential for establishing a simple, easy, convenient, and low-cost method for wastewater treatment as well as other environmental aspects.

ASSOCIATED CONTENT

Supporting Information

The Supporting Information is available free of charge at https://pubs.acs.org/doi/10.1021/acsomega.4c09763.

Characterization data for compounds **1**−**6** including ^1H and ^{13}C NMR, FT-IR and HRMS spectral data, and adsorption kinetics data for octols **1**−**4**. Kinetic and isotherm studies. A comparison between the results attained in this work with other reported adsorbents on MB removal from aqueous media (PDF).

https://doi.org/10.1021/acsomega.4c09763
ACS Omega 2025, 10, 12014−12025

AUTHOR INFORMATION

Corresponding Author

Ali Husain − *Department of Chemistry, Kuwait University, Safat 13060, Kuwait;* orcid.org/0000-0001-5150-6317; Email: ali.husain@ku.edu.kw

Authors

Mohamed Rashad − *Department of Chemistry, Kuwait University, Safat 13060, Kuwait*

Abrar Alrashed − *Department of Chemistry, Kuwait University, Safat 13060, Kuwait*

Abdullah Alhendal − *Department of Chemistry, Kuwait University, Safat 13060, Kuwait;* orcid.org/0000-0002-5438-2230

Maryam Jamali − *Department of Chemistry, Kuwait University, Safat 13060, Kuwait*

Saad Makhseed − *Department of Chemistry, Kuwait University, Safat 13060, Kuwait;* orcid.org/0000-0002-3239-5524

Complete contact information is available at: https://pubs.acs.org/10.1021/acsomega.4c09763

Author Contributions

The manuscript was written through contributions of all authors. All authors have given approval to the final version of the manuscript.

Notes

The authors declare no competing financial interest.

ACKNOWLEDGMENTS

The authors sincerely acknowledge Kuwait University, RSPU Facilities No. (GS 01/01, GS 01/03, GS 02/01, GS 03/01, GS 01/05, GS 02/13) and the National Unit for Environmental Research and Services (NUERS) (SRUL 01/13).

ABBREVIATIONS

NMR, nuclear magnetic resonance; FT-IR, Fourier-transform infrared spectroscopy; DSC, differential scanning calorimeters; ESI, electrospray ionization; SEM, scanning electron microscope; XPS, X-ray photoelectron spectrometer; TLC, thin layer chromatography; BTB, bromothymol blue; MV, methyl violet; MR, methyl red; CA, carminic acid; EBT, Eriochrome black T; DCF, dichlorofluorescein; DMF, *N,N*-dimethylformamide

REFERENCES

(1) Maheshwari, K.; Agrawal, M.; Gupta, A. B. *Dye Pollut. Water Wastewater* **2021**, 1−25.

(2) Islam, T.; Repon, M. R.; Islam, T.; Sarwar, Z.; Rahman, M. M. Impact of Textile Dyes on Health and Ecosystem: A Review of Structure, Causes, and Potential Solutions. *Environ. Sci. Pollut. Res.* **2023**, *30* (4), 9207−9242.

(3) Kiernan, J. Classification and Naming of Dyes, Stains and Fluorochromes. *Biotechnol. Histochem.* **2001**, *76* (5−6), 261−278.

(4) Elias, B.; Guihard, L.; Nicolas, S.; Fourcade, F.; Amrane, A. Effect of Electro-Fenton Application on Azo Dyes Biodegradability. *Environ. Prog. Sustainable Energy* **2011**, *30* (2), 160−167.

(5) Groeneveld, I.; Kanelli, M.; Ariese, F.; van Bommel, M. R. Parameters That Affect the Photodegradation of Dyes and Pigments in Solution and on Substrate − An Overview. *Dyes Pigm.* **2023**, *210*, No. 110999.

(6) Adesibikan, A. A.; Emmanuel, S. S.; Olawoyin, C. O.; Ndungu, P. Cellulosic Metallic Nanocomposites for Photocatalytic Degradation of Persistent Dye Pollutants in Aquatic Bodies: A Pragmatic Review. *J. Organomet. Chem.* **2024**, *1010*, No. 123087.

(7) Mim, S.; Hashem, M. A.; Maoya, M. Adsorption-Oxidation Process for Dyestuff Removal from Tannery Wastewater. *Environ. Nanotechnol., Monit. Manage.* **2024**, *21*, No. 100911.

(8) Zourif, A.; Benbiyi, A.; Kouniba, S.; El Guendouzi, M. Avocado Seed as a Natural Coagulant for Removing Dyes and Turbidity from Wastewater: Behnken Box Design, Sustainable Reuse, and Economic Evaluation. *Sustainable Chem. Pharm.* **2024**, *39*, No. 101621.

(9) Zhang, Q.; Cheng, Y.; Liu, C.; Fang, C. Electrochemical-Driven Removal of Organic Dyes by Using Bimetallic MOFs /Waste Cellulose Acetate Derived Carbon Foam as a Freestanding Electrode Material. *J. Solid State Chem.* **2024**, *330*, No. 124489.

(10) Tcheka, C.; Conradie, M. M.; Assinale, V. A.; Conradie, J. Mesoporous Biochar Derived from Egyptian Doum Palm (Hyphaene Thebaica) Shells as Low-Cost and Biodegradable Adsorbent for the Removal of Methyl Orange Dye: Characterization, Kinetic and Adsorption Mechanism. *Chem. Phys. Impact* **2024**, *8*, No. 100446.

(11) Kallawar, G. A.; Bhanvase, B. A. A Review on Existing and Emerging Approaches for Textile Wastewater Treatments: Challenges and Future Perspectives. *Environ. Sci. Pollut. Res.* **2024**, *31* (2), 1748−1789.

(12) Han, X. -N.; Han, Y.; Chen, C. -F. Recent Advances in the Synthesis and Applications of Macrocyclic Arenes. *Chem. Soc. Rev.* **2023**, *52* (9), 3265−3298.

(13) Liu, Z.; Nalluri, S. K. M.; Stoddart, J. F. Surveying Macrocyclic Chemistry: From Flexible Crown Ethers to Rigid Cyclophanes. *Chem. Soc. Rev.* **2017**, *46* (9), 2459−2478.

(14) Kharazmi, A.; Ghorbani-Vaghei, R.; Khazaei, A.; Karakaya, I.; Karimi-Nami, R. A Cost-Efficient Method for Green Synthesis of Novel Derivatives Lower-Rim-Connected Bisresorcinarene Macrocycles in Large-Scale by Sodium p-Styrenesulfonate. *Curr. Res. Green Sustainable Chem.* **2024**, *8*, No. 100396.

(15) Li, D.; Wu, G.; Zhu, Y. K.; Yang, Y. W. Phenyl-Extended Resorcin[4]Arenes: Synthesis and Highly Efficient Iodine Adsorption. *Angew. Chem., Int. Ed.* **2024**, *136* (43), No. e202411261.

(16) Tero, T. R.; Nissinen, M. A Perspective to Resorcinarene Crowns. *Tetrahedron* **2014**, *70* (6), 1111−1123.

(17) Kingsbury, C. J.; Senge, M. O. Molecular Symmetry and Art: Visualizing the Near-Symmetry of Molecules in Piet Mondrian's De Stijl. *Angew. Chem., Int. Ed.* **2024**, *63* (25), No. e202403754.

(18) Jen, A.; Merkle, H. P. Diamonds in the Rough: Protein Crystals from a Formulation Perspective. *Pharm. Res.* **2001**, *18* (11), 1483−1488.

(19) Patel, N.; Modi, K.; Bhatt, K.; Mohan, B.; Parikh, J.; Liska, A.; Ludvik, J.; Patel, C.; Jain, V. K.; Mishra, D. Cyclotriveratrylene (CTV): Rise of an Untapped Supramolecular Prodigy Providing a New Generation of Sensors. *J. Mol. Struct.* **2023**, *1273*, No. 134330.

(20) Mondal, P.; Rath, S. P. Cyclic Metalloporphyrin Dimers: Conformational Flexibility, Applications and Future Prospects. *Coord. Chem. Rev.* **2020**, *405*, No. 213117.

(21) La Manna, P.; Soriente, A.; De Rosa, M.; Buonerba, A.; Talotta, C.; Gaeta, C.; Neri, P. Green, Mild, and Efficient Friedel−Crafts Benzylation of Scarcely Reactive Arenes and Heteroarenes under On-Water Conditions. *ChemSusChem* **2019**, *12* (8), 1673−1683.

(22) Higler, I.; Boerrigter, H.; Verboom, W.; Kooijman, H.; Spek, A. L.; Reinhoudt, D. N. A Modular Approach to Potential Synthetic Receptors with Large Surfaces Based on Crown[n]Cavitands. *Eur. J. Org. Chem.* **1998**, *1998* (8), 1597−1607.

(23) Sala, P. D.; Vanni, C.; Talotta, C.; Di Marino, L.; Matassini, C.; Goti, A.; Neri, P.; Šesták, S.; Cardona, F.; Gaeta, C. Multivalent Resorcinarene Clusters Decorated with DAB-1 Inhitopes: Targeting Golgi α-Mannosidase from: Drosophila Melanogaster. *Org. Chem. Front.* **2021**, *8* (23), 6648−6656.

(24) Wang, Y. X.; Bi, Y. P.; Cui, Y. Y.; Yang, C. X. Synthesis of Crown Ether-Based Microporous Organic Networks: A New Type of Efficient Adsorbents for Chlorophenols. *J. Hazard. Mater.* **2023**, *443*, No. 130268.

(25) Brothers, P. J.; Ghosh, A.Coordination Chemistry. In *Fundamentals of Porphyrin Chemistry: A 21st Century Approach: Volume 1 and Volume 2*; Wiley, 2022; Vol. *1*−*2*, pp 141−240.

(26) Kumari, H.; Deakyne, C. A.; Atwood, J. L. Macrocyclic Coordination Chemistry of Resorcin[4]Arenes and Pyrogallol[4]-Arenes. *Macrocyclic Supramol. Chem.* **2016**, 325−345.
(27) Sun, H.; Sun, Z.; Wang, X. B. Probing Noncovalent Interaction Strengths of Host-Guest Complexes Using Negative Ion Photoelectron Spectroscopy. *Chem. - Eur. J.* **2024**, *30* (66), No. e202402766.
(28) Latha, A. T.; Swamy, P. C. A. Recent Advancements in Encapsulation of Poly Aromatic Hydrocarbons via Macrocyclic Host-Guest Chemistry. *Results Chem.* **2024**, *8*, No. 101588.
(29) Zhu, H.; Chen, L.; Sun, B.; Wang, M.; Li, H.; Stoddart, J. F.; Huang, F. Applications of Macrocycle-Based Solid-State Host−Guest Chemistry. *Nat. Rev. Chem.* **2023**, *7* (11), 768−782.
(30) Husain, A. A.; Bisht, K. S. Synthesis of a Novel Resorcin[4]-Arene-Glucose Conjugate and Its Catalysis of the CuAAC Reaction for the Synthesis of 1,4-Disubstituted 1,2,3-Triazoles in Water. *RSC Adv.* **2019**, *9* (18), 10109−10116.
(31) Rogers, C. H.; Pradeep, A.; Galiano, L. A.; Kelley, S. A.; Varadharajan, R.; Belmore, K.; Whitt, L. M.; Li, Y.; Champagne, P. A.; Ramamurthy, V.; Blackstock, S. C. Dynamic Covalent and Noncovalent Assembly of O-Nitrosocumene in Organic Solvents and Water. *Chem. Commun.* **2024**, *60* (94), 13899−13902.
(32) Suleymanov, A. A.; He, Q.; Müller, P.; Swager, T. M. Highly Contorted Rigid Nitrogen-Rich Nanographene with Four Heptagons. *Org. Lett.* **2024**, *26* (25), 5227−5231.
(33) Danylyuk, O. Host−Guest Complexes in the Crystal Land: A Plethora of Crystal Forms and Crystallization Peculiarities. *Crystallogr. Rev.* **2024**, *30* (1), 5−30.
(34) Nizam, N. U. M.; Hanafiah, M. M.; Mahmoudi, E.; Halim, A. A.; Mohammad, A. W. The Removal of Anionic and Cationic Dyes from an Aqueous Solution Using Biomass-Based Activated Carbon. *Sci. Rep.* **2021**, *11* (1), No. 8623.
(35) Meili, L.; Lins, P. V. S.; Costa, M. T.; Almeida, R. L.; Abud, A. K. S.; Soletti, J. I.; Dotto, G. L.; Tanabe, E. H.; Sellaoui, L.; Carvalho, S. H. V.; Erto, A. Adsorption of Methylene Blue on Agroindustrial Wastes: Experimental Investigation and Phenomenological Modelling. *Prog. Biophys. Mol. Biol.* **2019**, *141*, 60−71.
(36) Pang, J.; Fu, F.; Ding, Z.; Lu, J.; Li, N.; Tang, B. Adsorption Behaviors of Methylene Blue from Aqueous Solution on Mesoporous Birnessite. *J. Taiwan Inst. Chem. Eng.* **2017**, *77*, 168−176.
(37) Kumar, P.; Abbas, Z.; Kumar, P.; Das, D.; Mobin, S. M. Highlights in Interface of Wastewater Treatment by Utilizing Metal Organic Frameworks: Purification and Adsorption Kinetics. *Langmuir* **2024**, *40* (10), 5040−5059.
(38) Shokri, R.; Vonau, F.; Cranney, M.; Aubel, D.; Narladkar, A.; Isare, B.; Bouteiller, L.; Simon, L.; Reiter, G. Consequences of Varying Adsorption Strength and Adding Steric Hindrance on Self-Assembly of Supramolecular Polymers on Carbon Substrates. *J. Phys. Chem. C* **2012**, *116* (40), 21594−21600.
(39) Ferhan, A. R.; Jackman, J. A.; Cho, N. J. Investigating How Vesicle Size Influences Vesicle Adsorption on Titanium Oxide: A Competition between Steric Packing and Shape Deformation. *Phys. Chem. Chem. Phys.* **2017**, *19* (3), 2131−2139.
(40) Skala, L. P.; Yang, A.; Klemes, M. J.; Xiao, L.; Dichtel, W. R. Resorcinarene Cavitand Polymers for the Remediation of Halomethanes and 1,4-Dioxane. *J. Am. Chem. Soc.* **2019**, *141* (34), 13315−13319.
(41) El Jery, A.; Alawamleh, H. S. K.; Sami, M. H.; Abbas, H. A.; Sammen, S. S.; Ahsan, A.; Imteaz, M. A.; Shanableh, A.; Shafiquzzaman, M.; Osman, H.; Al-Ansari, N. Isotherms, Kinetics and Thermodynamic Mechanism of Methylene Blue Dye Adsorption on Synthesized Activated Carbon. *Sci. Rep.* **2024**, *14* (1), No. 970.
(42) Kazakova, E. K.; Morozova, J. E.; Prosvirkin, A. V.; Pich, A. Z.; Gubanov, E. P.; Muslinkin, A. A.; Habicher, W. D.; Konovalov, A. I. Self-Assembly of Octaaminoamido Derivatives of Resorcin[4]Arene in Water - A "Cell-like" Submicron-Scale Hydrogel Structure. *Eur. J. Org. Chem.* **2004**, *2004* (15), 3323−3329.
(43) Shalaeva, Y. V.; Morozova, J. E.; Syakaev, V. V.; Kazakova, E. K.; Ermakova, A. M.; Nizameev, I. R.; Kadirov, M. K.; Konovalov, A. I. Supramolecular Nanoscale Systems Based on Amphiphilic Tetramethylensulfonatocalix[4]Resorcinarenes and Cationic Polyelectrolyte with Controlled Guest Molecule Binding. *Supramol. Chem.* **2017**, *29* (4), 278−289.
(44) Sivakumar, R.; Yoon, N. Adsorptive Removal of Organic Pollutant Methylene Blue Using Polysaccharide-Based Composite Hydrogels. *Chemosphere* **2022**, *286*, No. 131890.

https://doi.org/10.1021/acsomega.4c09763
ACS Omega 2025, 10, 12014−12025